nature immunology

Identification of amino acid residues crucial for chemokine receptor dimerization

Patricia Hernanz-Falcón[1], José Miguel Rodríguez-Frade[1,3], Antonio Serrano[1,3], David Juan[2], Antonio del Sol[2], Silvia F Soriano[1], Fernando Roncal[1], Lucio Gómez[1], Alfonso Valencia[2], Carlos Martínez-A[1] & Mario Mellado[1]

Chemokines coordinate leukocyte trafficking by promoting oligomerization and signaling by G protein–coupled receptors; however, it is not known which amino acid residues of the receptors participate in this process. Bioinformatic analysis predicted that Ile52 in transmembrane region-1 (TM1) and Val150 in TM4 of the chemokine receptor CCR5 are key residues in the interaction surface between CCR5 molecules. Mutation of these residues generated nonfunctional receptors that could not dimerize or trigger signaling. *In vitro* and *in vivo* studies in human cell lines and primary T cells showed that synthetic peptides containing these residues blocked responses induced by the CCR5 ligand CCL5. Fluorescence resonance energy transfer showed the presence of preformed, ligand-stabilized chemokine receptor oligomers. This is the first description of the residues involved in chemokine receptor dimerization, and indicates a potential target for the modification of chemokine responses.

The chemokines are a large family of proteins that regulate recruitment of leukocytes to sites of inflammation and coordinate their trafficking throughout the body[1]. Chemokines mediate leukocyte function by binding to and activating specific G protein–coupled receptors (GPCRs) expressed by these cell populations[2]. Ligand binding to the GPCR promotes the association and activation of Janus tyrosine kinases (JAKs)[3] and stimulates GDP-GTP exchange in the G protein $G\alpha_i$ subunit. Although these receptors were initially believed to be monomers, a growing body of evidence shows GPCR oligomerization, indicating the complexity of GPCR activation and signaling in the cell[4–8]. Several models have been proposed for GPCR dimerization[9]. Some GPCRs, such as the metabotropic glutamate receptor-1 (ref. 10), have long extracellular N-terminal extensions that bind ligands and contribute to dimer stabilization. Others, such as the γ-aminobutyric acid (B) ($GABA_B$) receptor, dimerize through coiled-coil domain interaction within the C-terminal tails[11]. For the β-adrenergic receptor, ligand-induced signal transduction requires interaction between the seven-transmembrane helices, where the key residues are found[5], as has also been observed for the δ-μ opioid receptor[12].

Using a variety of approaches, several groups[13–17] have described chemokine receptor dimerization and its influence on receptor function[18]. Monoclonal antibodies (mAb) to CCR5 (anti-CCR5) stabilize multiple active states of the CCR5 receptor[16]. In addition, we have reported activation of distinct signaling events by chemokine receptor homo- or heterodimers[18] and have found that CCR5 dimers influence susceptibility of primary cells to HIV-1 infection[19]. The biological significance of GPCR dimerization is poorly characterized, however, and both the dimerization site and the amino acid residues involved in this process remain to be elucidated. Through a combination of *in silico* analysis, imaging techniques, biochemistry, and *in vitro* and *in vivo* functional analyses, we have identified two crucial amino acid residues involved in CCR5 dimerization, and we describe their possible application as tools to block chemokine responses.

RESULTS

Ile52 and Val150 are essential for CCR5 function

Based on amino acid sequence alignment, we used bioinformatic analysis that detects compensatory mutations[20,21] and family-specific residues[22,23] to identify a protein region crucial for chemokine receptor dimerization; this region is predicted to include a large part of the transmembrane regions TM1 and TM4. To visualize the structural implications of these predictions, we used the Global Range Molecular Matching docking program and a low-resolution representation of the CCR5 TM regions to build models of a homodimer structure compatible with the predicted contact interface. This model positions the basic structure for homodimer formation at the interaction site between TM1 and TM4 (**Fig. 1**).

On the basis of these predictions for the CCR5 interaction sites, we explored the dimerization model by analyzing mutants with alterations of the contact amino acid residues. Of all possibilities analyzed, a two-point mutation in this theoretical CCR5 contact network, resulting in I52V and V150A substitutions, appeared crucial and was evaluated in detail. We generated the CCR5 double mutant CCR5I52VV150A (CCR5mut) and stably transfected either wild-type

[1]Department of Immunology and Oncology and [2]Protein Design Group, National Center of Biotechnology, Campus Universitario de Cantoblanco, E-28049 Madrid, Spain. [3]These authors contributed equally to this work. Correspondence should be addressed to C.M.-A. (cmartineza@cnb.uam.es).

Published online 11 January 2004; doi:10.1038/ni1027

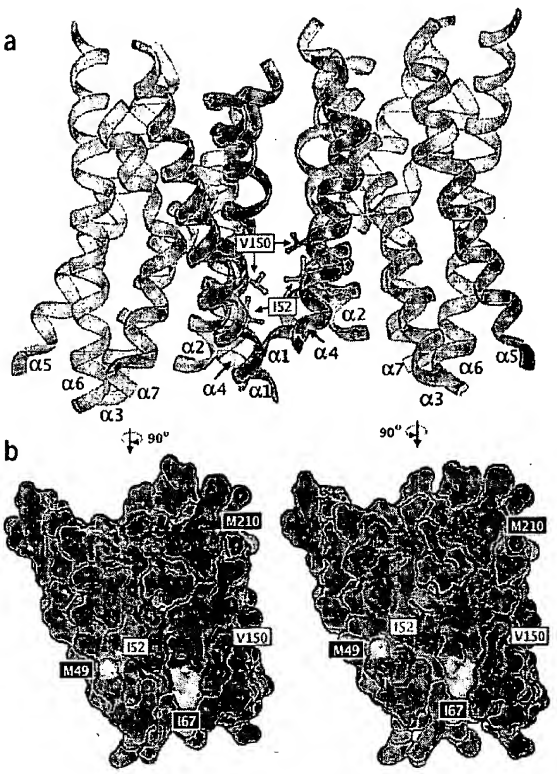

Figure 1 Structural model of CCR5 dimer association. (**a**) Ribbon representation of CCR5 transmembrane domains TM1, TM2 and TM4 (α1, α2 and α4), which participate directly in the interaction surface. Mutated residues Ile52 and Val150 are indicated. (**b**) Interaction surface in the two monomers. The residues that form part of the interaction surface are colored magenta, those predicted to be important for interaction specificity are in yellow and mutated residues are in red.

CCR5 (CCR5wt) or CCR5mut into the L1.2 mouse pre-B cell line. Both receptors were expressed equally on the cell membrane, as shown by anti-CCR5 staining (**Fig. 2a**, upper). They bind similar amounts of ligand in flow cytometry with biotin-labeled CCL5 (**Fig. 2a**, lower) with similar affinity constants, as indicated by Scatchard analysis (**Fig. 2b**) (0.88 ± 0.22 nM, CCR5wt; 1.33 ± 0.33 nM, CCR5mut).

Evaluation of receptor function showed that CCR5wt responded to CCL5 in chemotaxis (**Fig. 2c**) and calcium mobilization assays (**Fig. 2d**), whereas CCR5mut did not respond to the ligand at any concentration tested. As a control, both cell types responded equally to CXCL12 activation through the endogenous CXCR4 (**Fig. 2c,d**). We have reported previously that JAK association to the receptor and receptor dimerization are the first events that follow chemokine binding[3,17]. Thus, we evaluated these steps in CCR5wt and CCR5mut cells. JAK2 bound to CCR5wt after CCL5 activation, with normal association kinetics, as indicated by its detection in CCR5wt immunoprecipitates (**Fig. 2e**, left), but it did not bind to CCR5mut (**Fig. 2e**, right). This result indicates that no signaling events are triggered through the mutant receptor. As predicted, signal transducer and transactivator of transcription (STAT) factors were not observed in CCR5mut immunoprecipitates (**Fig. 2f**, right), whereas CCR5wt showed complete JAK-STAT activation (**Fig. 2f**, left).

To analyze whether this model could be extended to other chemokine receptors, we used the same approach to predict that Val64 in TM1 and Ile164 in TM4 are the residues involved in the CCR2 dimerization site. We generated the CCR2 double mutant CCR2V64AV164A (CCR2mut), and stably transfected wild-type CCR2 (CCR2wt) or CCR2mut into the L1.2 mouse pre-B cell line. CCR2mut did not respond to CCL2 in calcium or in chemotaxis assays at any ligand concentration tested, although these cells responded appropriately to CXCL12 stimulation (see **Supplementary Fig. 1** online).

As CCR5 signaling is reported to take place in raft microdomains[24], the lack of function of CCR5mut may be due to altered receptor localization on the cell membrane. We costained cells to detect CCR5wt or CCR5mut and the cholera toxin β-subunit (CTx), a marker specific for the raft-associated glycosphingolipid GM1. Both forms of CCR5 colocalized with CTx (see **Supplementary Fig. 2** online), indicating that the lack of CCR5mut function is not due to differences in membrane distribution. The specificity of CCR5wt and CCR5mut raft aggregation was confirmed by mAb cross-linking of the transferrin receptor (TfR), a protein excluded from membrane rafts[25], showing that anti-TfR–induced staining does not colocalize with that observed with CTx (**Supplementary Fig. 2** online). Although CCR5mut and CCR5wt raft location and ligand binding characteristics were indistinguishable, the data indicate that CCR5mut was unable to signal.

The CCR5I52VV150A mutant receptor does not dimerize

As receptor dimerization is required for correct chemokine signaling[3], we evaluated receptor dimerization in CCR5wt and CCR5mut cells. Unstimulated or CCL5-stimulated transfected cells were cross-linked with disuccinimidyl suberate (DSS) before lysis, cell extracts were immunoprecipitated with anti-CCR5, and immunoblots were developed with CCR5 mAb. A band corresponding to CCR5 monomer was detected in both cases, independently of CCL5 activation (**Fig. 3a**). However, higher-molecular-weight species equivalent to dimers and oligomers were detected in CCR5wt (**Fig. 3a**, left) but not in CCR5mut cells (**Fig. 3a**, right) after CCL5 stimulation.

In these experiments, CCR5wt dimers were detected only after ligand activation, in agreement with previous reports[18]. Some recent studies have detected several chemokine receptor conformations, indicating that oligomerization may take place even in the absence of ligand stimulation[14,15]. To analyze the role of the ligand in this process, we used fluorescence resonance energy transfer (FRET), a method that permits temporal and spatial resolution of dimerization by detecting acceptor fluorescence after donor excitation[26].

HEK-293 cells were transiently cotransfected with CCR5wt–cyan fluorescent protein (CFP; donor) and CCR5wt–yellow fluorescent protein (YFP; acceptor) (R5wt-C–R5wt-Y) or with CCR5mut-CFP and CCR5mut-YFP (R5mut-C–R5mut-Y). FRET was detected in unstimulated R5wt-C–R5wt-Y cells but not in R5mut-C–R5mut-Y cells (**Fig. 3b**). These data are in agreement with the immunoblot results indicating that CCR5mut does not dimerize, and confirm the observations that chemokine receptors exist as preformed dimers, even in the absence of ligand. The apparent discrepancy with immunoblot data may be due to differences in technique sensitivity.

To evaluate this effect more precisely, FRET was quantified by sensitized acceptor fluorescence[27] in unstimulated or CCL5-stimulated R5wt-C–R5wt-Y or R5mut-C–R5mut-Y cells. Basal FRET energy was detected in CCR5wt transfectants, and increased after addition of CCL5 (**Fig. 3c**). In contrast, CCR5mut transfectants showed neither basal nor CCL5-mediated FRET, despite cell surface expression of CCR5mut. The data indicate that CCR5mut does not dimerize and that FRET is not a consequence of receptor overexpression. An evaluation of dimerization using fluorescence lifetime imaging (FLIM)

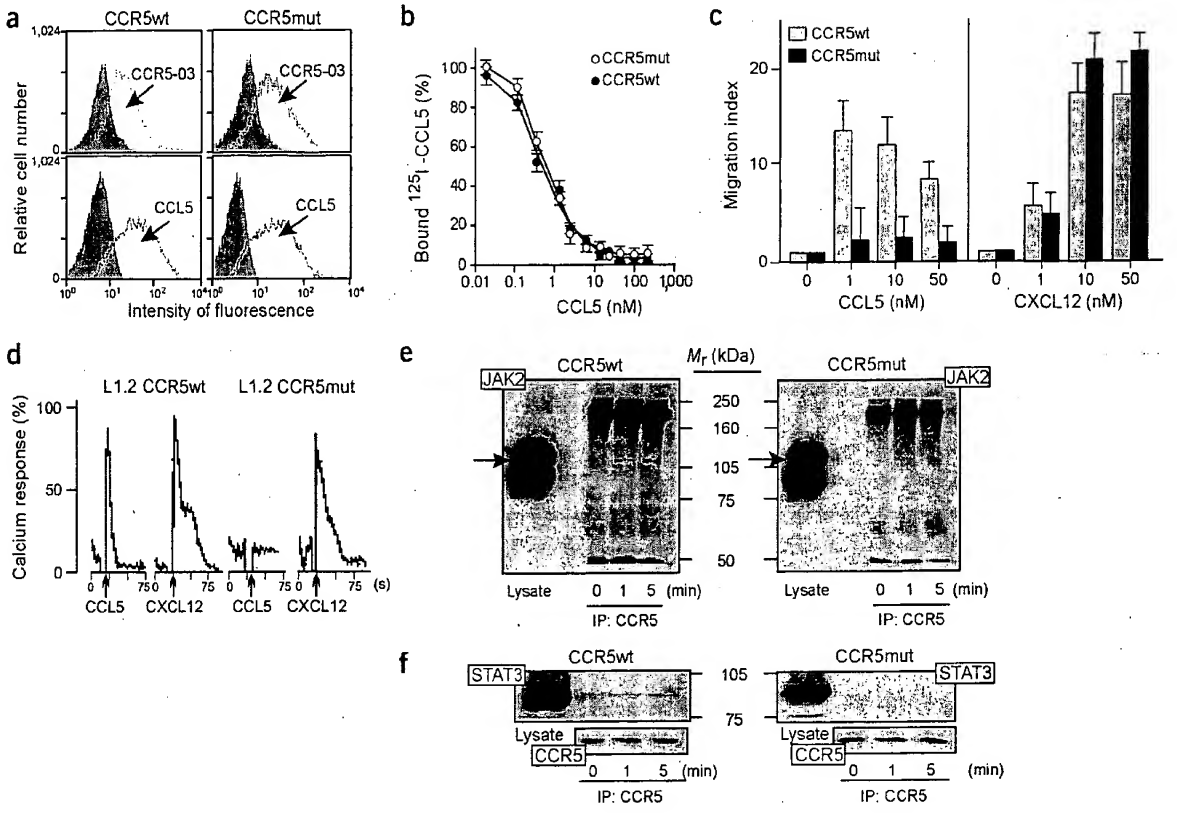

Figure 2 I52V and V150A point mutations in CCR5 abrogate receptor function. (**a**) CCR5wt and CCR5mut expression in transfected L1.2 cells was measured by flow cytometry with biotin-labeled CCR5-03 mAb (upper) or biotin-labeled CCL5 (lower), followed by FITC-streptavidin. (**b**) Displacement curve of CCL5 competitive binding for ^{125}I-labeled CCL5 on CCR5wt– and CCR5mut–stably transfected L1.2 cells. Data represent the mean of triplicate determinations from one experiment of five performed. (**c**) Migration of CCR5wt- and CCR5mut-transfected L1.2 cells in response to CCL5 or CXCL12. Cells that migrated to the lower chamber were counted and expressed as a migration index. Data represent the mean ± s.d. of triplicate determinations from one experiment of ten performed. (**d**) CXCL12- or CCL5-induced calcium mobilization in CCR5wt- and CCR5mut-transfected L1.2 cells was measured by flow cytometry. (**e**) CCL5 (20 nM)-induced CCR5wt- or CCR5mut-transfected L1.2 cell lysates were immunoprecipitated with anti-CCR5 and immunoblotted with anti-JAK2. As a positive control, unprecipitated L1.2 cell lysates were tested with anti-JAK2. (**f**) CCL5 (20 nM)-induced CCR5wt- or CCR5mut-transfected L1.2 cell lysates were immunoprecipitated as in **e** and the immunoblot developed with anti-STAT3. Equivalent receptor loading was confirmed by reprobing with CCR5-01 mAb. As a positive control, unprecipitated L1.2 cell lysates were tested with anti-STAT3. All immunoblots show one representative experiment of at least five performed.

technology produced identical conclusions[28]. FLIM measures the specific CFP lifetime, which decreases owing to energy capture when CFP is in proximity to YFP molecules. We evaluated homodimerization of CCR5 by FLIM using the same transfectants as in the FRET experiments. In individually transfected control R5wt-C and R5mut-C cells, the lifetime of CFP was 2.10 ± 0.01 ns; this was reduced to 1.8 ± 0.02 ns in R5wt-C–R5wt-Y cells, confirming CCR5wt homodimerization (**Fig. 3d,e**). When this experiment was carried out with R5mut-C–R5mut-Y cells, no significant reduction was observed in CFP lifetime (2.05 ± 0.01 ns), confirming the absence of homodimerization observed with FRET (**Fig. 3d,e**).

We showed previously that CCR5 can heterodimerize with CCR2 and that the resulting receptor complex activates signaling events distinct from those triggered by the homodimers[18]. To test whether CCR5mut is able to associate with CCR2, we transiently cotransfected HEK-293 cells cotransfected with CCR2wt–cyan fluorescent protein (R2wt-C) and CCR5wt–yellow fluorescent protein (R5wt-Y) (R2wt-C–R5wt-Y), or R2wt-C and CCR5mut-Y (R2wt-C–R5mut-Y), then evaluated them with FLIM for the presence of preformed heterodimers. CFP lifetime was 2.1 ± 0.02 ns in R2wt-C cells but was reduced to 1.7 ± 0.05 ns in R2wt-C–R5wt-Y cells (see **Supplementary Fig. 3** online), confirming CCR5–CCR2 heterodimerization. When this experiment was done with R2wt-C–R5mut-Y cells, no significant reduction was observed in CFP lifetime (2.05 ± 0.01 ns) (**Supplementary Fig. 3** online). Heterodimerization was more evident in the cell membrane of R2wt-C–R5wt-Y cells, suggesting that this process occurs in specific areas. Similar to other GPCRs[29], chemokine receptors appear to be in monomer, dimer and oligomer equilibrium, and the ligand may stabilize the active receptor conformation. Thus, mutation of CCR5 Ile52 in TM1 and Val150 in TM4 results in disruption of the dimer, indicating a key role for these residues in CCR5 dimerization.

Synthetic peptides block CCR5 function

Because mutation of CCR5 residues Ile52 and Val150 impeded the receptor's function by preventing dimerization, we considered that competition for the contact sites could also block CCR5 signaling. We designed seven-amino-acid synthetic peptides containing the key

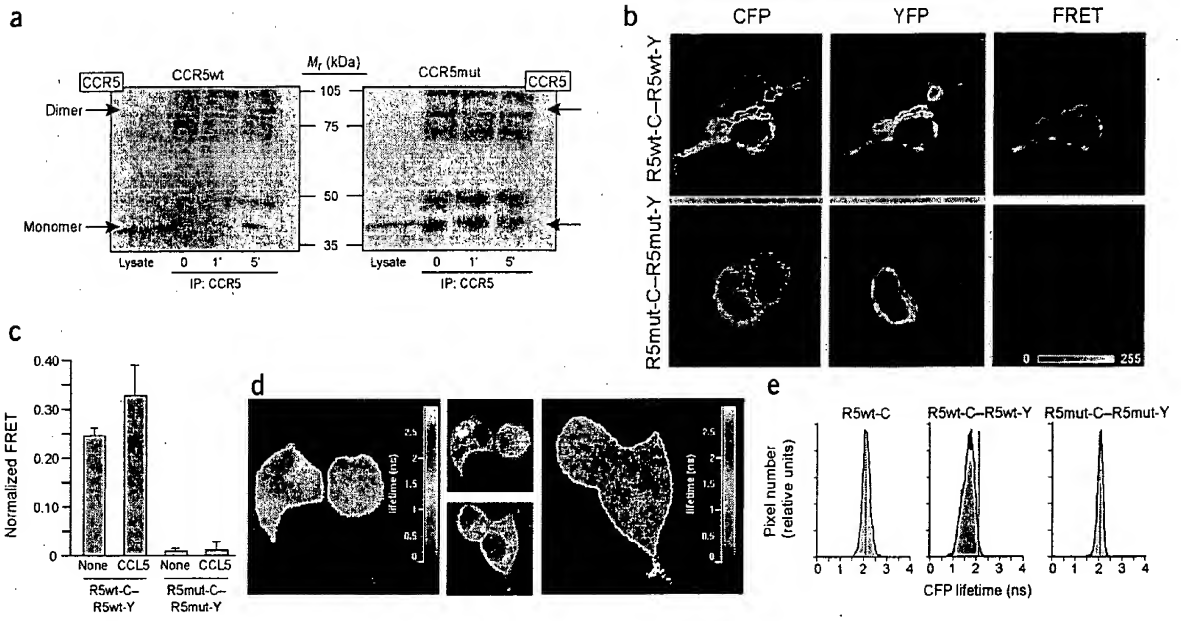

Figure 3 CCL5 does not trigger CCR5mut dimerization. (**a**) Serum-starved CCR5wt- or CCR5mut-transfected L1.2 cells were left unstimulated or stimulated with 20 nM CCL5, then cross-linked with DSS. Cell lysates were immunoprecipitated with CCR5-03 and then immunoblotted with CCR5-01. As a control, lysates from un-cross-linked CCR5wt- or CCR5mut-transfected L1.2 cells were immunoblotted with the same CCR5 mAb. Arrows indicate receptor monomer and dimer. (**b**) Unstimulated R5wt-C–R5wt-Y (upper) or R5mut-C–R5mut-Y (lower) HEK-293 cells were visualized with filter sets for CFP (left) and for YFP (middle). FRET images (right) were visualized with the FRET filter set, expressed as corrected FRET (see Methods) and displayed in quantitative pseudocolor (arbitrary linear units of fluorescence intensity). (**c**) R5wt-C–R5wt-Y or R5mut-C–R5mut-Y HEK-293 cells, unstimulated or stimulated with 20 nM CCL5, were fixed and FRET evaluated. Shown are normalized FRET values for 5 independent images of at least 15 cells each (see Methods). (**d**) CFP fluorescence lifetime images (calculated from the phase shift) of HEK-293 cells expressing R5wt-C–R5wt-Y (left) or R5mut-C–R5mut-Y (right). The pseudocolor scale ranges from 0 (black) to 3.0 ns (white). As controls, fluorescence images are shown for R5wt-C (middle, upper) and R5mut-C (middle, lower). (**e**) Histograms show the fluorescence lifetime distribution throughout the image for HEK-293 cells transiently transfected with R5wt-C (left), R5wt-C–R5wt-Y (middle) or R5mut-C–R5mut-Y (right). Red line shows the mean lifetime for R5wt-C.

residues involved in CCR5 dimerization. We synthesized Ile52-bearing (R5wt1; MLVILIL) and Val150-bearing peptides (R5wt4; VTSVITW), as well as control peptides with the I52V (R5mut1; MLVVLIL) and V150A mutations (R5mut4; VTSAITW). Peptides were also synthesized with an N-terminal biotin group to permit us to monitor their inclusion in the cell membrane. CCR5wt cells were incubated with biotin-labeled peptides, washed and developed with phycoerythrin-labeled streptavidin. All peptides were detected in the cell membrane, as shown by flow cytometric analysis (**Fig. 4a**) or by confocal microscopy with Cy2-streptavidin (data not shown). FRET analysis was carried out to evaluate whether the peptides disrupt CCR5 dimers. R5wt-C–R5wt-Y HEK-293 cells treated with R5wt1 plus R5wt4 (WT pep) or with R5mut1 plus R5mut4 (Mut pep) were fixed and FRET was evaluated by fluorescence microscopy as above. Preformed CCR5 homodimers were disrupted by treatment with peptides containing the intact CCR5 dimerization site, whereas

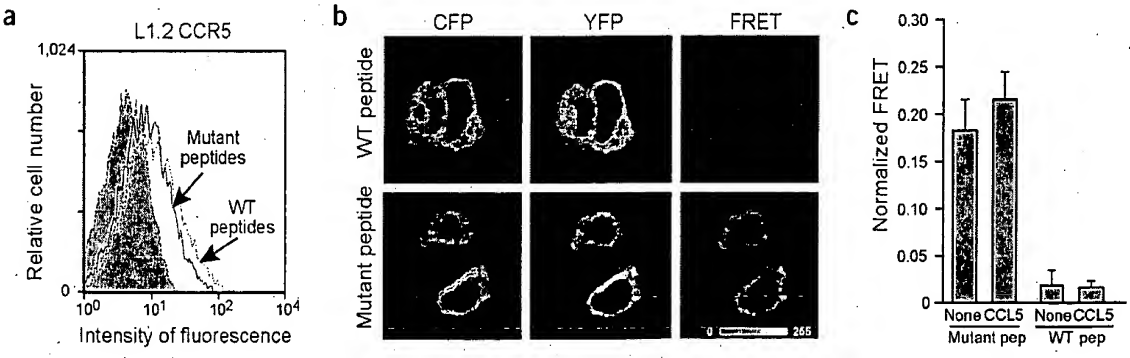

Figure 4 Synthetic peptides containing Ile52 and Val150 block CCR5 dimerization. (a) CCR5wt-transfected L1.2 cells were incubated with biotin-labeled synthetic peptides (WT pep or Mut pep) followed by FITC-streptavidin, and binding was analyzed by flow cytometry. (b) R5wt-C–R5wt-Y HEK-293 cells were treated with WT pep (upper) or Mut pep (lower) for 30-min, then analyzed as in **Figure 3b**. (c) Normalized FRET values were obtained as in **Figure 3c**.

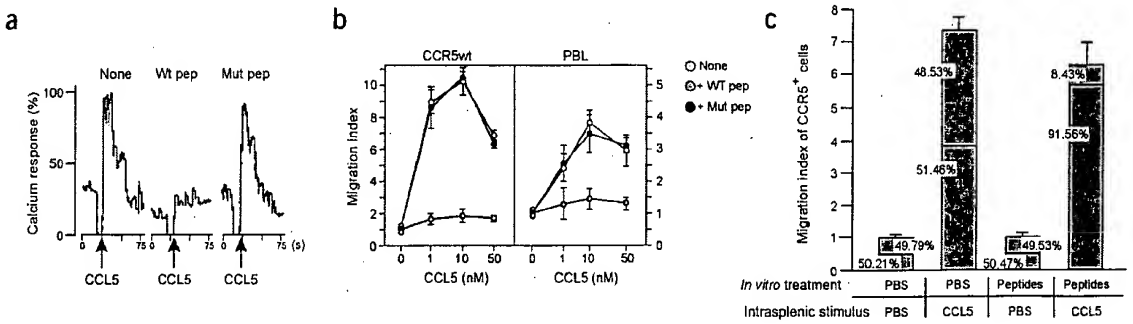

Figure 5 Synthetic peptides containing Ile52 and Val150 block CCR5-induced responses. (**a**) Flow cytometric analysis of CCL5-induced calcium mobilization in CCR5wt-transfected L1.2 cells either left untreated or treated with WT pep or Mut pep. (**b**) CCR5wt-transfected L1.2 cells (left) or PBLs from healthy donors (right) were treated with WT pep or Mut pep and allowed to migrate in response to CCL5. Cells that migrated to the lower chamber were counted and the number expressed as a migration index. Data represent the mean ± s.d. of triplicate determinations ($n = 5$). (**c**) PBLs from healthy donors were labeled with CT orange or green, and treated with WT pep (green), Mut pep (orange) or PBS (green and orange), injected intravenously into mice, and their accumulation in spleen analyzed after intrasplenic injection of CCL5. Results of three independent experiments are expressed as the migration index of $CCR5^+$ cells (mean ± s.d.) calculated as indicated in Methods. The figure also shows the ratio of orange- to green-stained cells for each condition.

peptides containing mutated residues did not alter CCR5 oligomerization (**Fig. 4b,c**).

To evaluate the effect of the peptides on CCR5 function, CCR5wt cells or peripheral-blood lymphocytes (PBLs) from healthy human donors were treated with WT pep or Mut pep, or left untreated, before CCL5 activation. WT pep–pretreated cells did not respond to CCL5 in calcium flux (**Fig. 5a**) or migration assays (**Fig. 5b**), whereas Mut pep–treated cells retained their ability to respond to ligand in both transfectants and primary cells (**Fig. 5a,b**). Flow cytometric analysis indicated that peptides affected neither cell surface receptor expression nor cell viability (data not shown). Peptide specificity was tested in functional assays with the unrelated muscarinic type-1 GPCR or with distinct chemokine receptors. Treatment of J-HM1-2.2 cells[30] with WT pep or Mut pep had no effect on carbachol-mediated calcium flux (see **Supplementary Fig. 4** online). In addition, peptide treatment had no effect on CCL17-, CCL20-, CCL1-, CCL25- or CCL27-induced calcium flux in HEK-293 cells stably transfected with hCCR4, hCCR6, hCCR8, hCCR9 or hCCR10, respectively (**Supplementary Fig. 4** online).

Similar results were obtained in analyses of *in vivo* responses to CCL5. Equal numbers of activated human PBLs expressing functional CCR5 were stained with CellTracker orange or green dye. Green-stained cells were treated with WT pep or PBS (control); orange-stained cells were treated with Mut pep or PBS. Subsequently, cell mixtures treated with PBS + PBS or with Mut pep + WT pep (1:1 orange/green) were injected intravenously into mice, which were then immediately injected intrasplenically with CCL5 or PBS. When cell accumulation in spleen was analyzed by flow cytometry 4 h after CCL5 injection, no alteration was observed in the initial 1:1 orange/green ratio for PBS-treated cells (48.53 ± 0.2%:51.46 ± 0.2%) (**Fig. 5c**). For peptide-treated cells, however, only Mut pep–treated (orange) cells accumulated in numbers similar to control cells in CCL5-injected mouse spleen, whereas WT pep–treated (green) cells did not (orange/green ratio 91.56 ± 0.3%:8.43 ± 0.3%) (**Fig. 5c**). Nonspecific orange/green cell accumulation in PBS-injected mice showed a 1:1 ratio under all treatment conditions (50.2 ± 0.1%:49.8 ± 0.1%).

The WT pep and the Mut pep were also tested for their ability to block CCL5-induced migration of activated human PBLs injected intravenously into the peritoneal cavity of mice. In this model, as for T cell migration to spleen, the WT pep blocks CCR5-triggered responses (data not shown). Altogether, the data indicate that chemokine responses are altered specifically by the presence of synthetic peptides that include the key dimerization residues Ile52 and Val150.

DISCUSSION

Dynamic protein-protein interactions are central components of biological regulatory networks. Among these interactions, dimerization events are a common mechanism for signal transduction from the cell surface to the nucleus, allowing the generation of considerable functional diversity. Protein dimerization occurs between a wide variety of cellular components, including cell surface receptors (tyrosine kinase receptors, cytokine receptors, antigen receptor), signaling molecules (Bcl-2 family, Smad family) and transcription factors (nuclear hormone receptors, STAT, basic helix-loop-helix proteins, BZIP family). In all these cases, dimerization allows activation and regulation of associated proteins. Dimerization may also enhance specificity, serve as a cellular mechanism to control sensitivity, or modulate activity by interaction with dominant-negative partners and regulatory proteins. The transition between monomeric and dimeric states is a regulated process, and in many cases is the rate-limiting step for activation[31].

G protein receptors, initially believed to be monomers, induce functional responses through receptor dimerization. Receptors such as β-adrenergic, muscarinic, GABA or chemokine receptors have been shown to be dimeric entities[32]. In these receptors, dimerization has a key role in several processes, including receptor trafficking to the cell membrane, specificity in signaling events, and sensitivity to chemotactic gradients. However, the role of the ligand in inducing or stabilizing receptor complexes remains controversial, and thus an effort is being made to identify the amino acid residues that define the dimerization site.

Bioinformatic analysis of the chemokine receptor family predicts that TM1, TM2 and TM4 are the principal domains involved in homodimer formation. Examination of the CCR5 model showed that two point mutations, I52V in TM1 and V150A in TM4, were sufficient to abrogate receptor function. The use of energy transfer techniques (FRET and FLIM) demonstrated that unlike wild-type CCR5, the double-mutant CCR5 was unable to dimerize even after ligand

stimulation. On the other hand, although ligand binding had an effect on dimerization of wild-type CCR5, the FRET value was modest, suggesting that the ligand did not drive dimerization but rather stabilized the dimeric conformation. However, the FRET index from untreated cells reflects receptor colocalization throughout the cell, whereas the measurable effect of the ligand is cell membrane-restricted. Thus, quenching from background receptor dimerization may mask the effect of the ligand on dimerization. FLIM analysis of wild-type CCR2-CCR5 heterodimers supported the hypothesis that the ligand induces dimerization by showing that the ligand modifies CFP lifetime specifically in the membrane.

Our results, which agree with other GPCR models[33], indicate that CCR5 oligomers are present in unstimulated cells and that the ligand induces and stabilizes the oligomeric conformation with the highest binding affinity. The CCR5 oligomers in unstimulated cells observed with FRET were not detected in immunoblot assays, possibly because dimer stability can be influenced by many factors, including detergents used to lyse cells for immunoprecipitation. In contrast, the presence of ligand, associated with conformational changes in GPCR structure[34], might stabilize the dimer in a conformation resistant to detergent treatment, allowing subsequent detection. In addition, CCR5 dimerization involves highly conserved epitopes in TM1 and TM4, which include residues Ile52 and Val150. Residues such as threonine and proline (in the TXP motif) that have been identified in other integral membrane proteins[35] are also found in the CCR5 TM2 helix, and appear to be crucial for correct receptor function[36]. Our data obtained with synthetic peptides indicate that the amino acid residues that surround Ile52 and Val150 could be very important in promoting peptide specificity for the receptor.

These results support our model, which requires GPCR structural integrity to preserve the backbone flexibility needed for the activation-associated conformational changes. The amino acids involved in dimerization are specific because CCR5-related synthetic peptides do not affect the function of other GPCR or chemokine receptors. However, this mechanism can be extrapolated to other chemokine receptors, as shown by the identification of residues involved in the CCR2 dimerization site. Thus, a CCR2 mutant bearing point mutations for V64A in TM1 and V164A in TM4 was unable to trigger receptor function.

Finally, our data also indicate that the monomeric conformation is an inactive receptor state, as it is unable to trigger function or to activate the steps that initiate chemokine signaling[37], such as the association with JAK. This observation may help to resolve the mechanism of JAK activation though chemokine receptors and other GPCRs.

We have shown that seven-amino-acid synthetic peptides containing the key CCR5 dimerization residues Ile52 and Val150 abrogate CCR5 function by disrupting CCR5 homodimers. Small peptides such as those described here can be considered a novel class of antagonists, because they act by preventing the stabilization of active receptor conformations. The hydrophobic nature of the transmembrane peptides greatly facilitates their penetration into the cell membrane bilayer, and their orientation within the membrane may be due to their capacity to dock to the receptor α-helix. The current search for antibodies or chemical compounds that neutralize chemokine effects has been based mainly on blockade of chemokine or chemokine-receptor binding sites[38]. Our results indicate that stabilization of an inactive chemokine receptor conformation is a potential target for therapeutic intervention. CCR5 mAb have been described that stabilize multiple active CCR5 conformations, each of which has distinct functional effects[16]. We propose that stabilizing an inactive chemokine receptor alters chemokine function, because selective receptor stabilization in the monomeric state would regulate the on-off switch of a specific chemokine receptor. Emphasis on the GPCR TM domains as targets for inhibitors is not new. For example, peptides that mimic TM helices and disrupt receptor function have been reported[39]. Potent antagonistic, low-molecular-weight chemical compounds have been described whose binding sites are located within the transmembrane bundle of the receptors[40,41]. One example is TAK-779, a small-molecule inhibitor of CCR5 function, whose binding site has been mapped to a cavity between TM1, TM2, TM3 and TM7 (ref. 40). Our results provide information on the key residues implicated in chemokine receptor dimerization, offer new possibilities for specific intervention in chemokine physiology, and define additional targets for the design of drugs with therapeutic potential in chemokine-related diseases.

METHODS

Prediction of the dimerization model. We used the GPCRDatabase[42] for multiple sequence alignments, as well as alignments derived with the TCOFFEE program[43].

Prediction of tree determinant residues. SequenceSpace[22] and other methods[23] were used to detect family-specific residues. We used comparative analysis of different chemokine receptor families to determine the presence of potential specific receptor interaction sites. Because of its greater sequence diversity, the CXCR family was analyzed first and the results projected onto the full CCR–CXCR alignment. Details of SequenceSpace analysis and the residues specific for each family split are available as a **Supplementary Note** online.

Prediction of protein interaction regions based on detection of correlated pairs of positions. To detect correlated positions in multiple sequence alignments, we used the algorithm developed by Gobel *et al.*[20], extended for protein interaction prediction[21]. A similar approach was developed independently by Filizola *et al.*[44] for GPCRs. The basic principle is that accumulation of complementary variations between sequences of interacting proteins can be distinguished from background levels of sequence variation. Application of this method to the detection of homodimers requires additional differentiation between predicted intra- and intermolecular interactions. We used residues predicted to have a surface exposure of more than 50 $Å^2$ as an indicator of potential implication in interprotein interactions.

Construction of a structural model for receptor dimerization. A low-resolution, three-dimensional model of the CCR5 chemokine receptor was taken from the GPCR database (http://www.cmbi.kun.nl/7tm/); it corresponds to a model based on the low-resolution map of rhodopsin[45]. Loop regions are intentionally excluded, because the rhodopsin framework does not provide information for their modeling. These models should be interpreted as purely topological; gross divergence from the true structure is anticipated.

The potential homodimer model was selected from among a large number of alternative structures built with the low-resolution Global Range Molecular Matching (GRAMM) docking method[46,47]. The solutions that maintain correct membrane orientation were further classified by proximity of the correlated residue pairs and/or family-specific residues. A similar procedure applied to a large protein collection showed good correlation between model accuracy and proximity of correlated pairs[48].

Site-directed mutagenesis of CCR5 Ile52 and Val150. For CCR5, isoleucine was replaced by valine at residue 52 and valine was replaced by alanine at residue 150. For CCR2, valine was replaced by alanine at residue 64 and valine was replaced by alanine at residue 164. In both cases we used the QuickChange site-directed mutagenesis kit (Stratagene, Germany) and manufacturer's protocols. The two oligonucleotide primers synthesized for CCR5 correspond to positions 139–171 and 433–465; the first contains the target isoleucine codon (ATC) at position 154, which was replaced with a valine codon (GTC); the second contains the target valine codon (GTG) at position 448, which was replaced with an alanine codon (GCG). For CCR2, the primers correspond to positions 174–201 and 468–501; the first contains the target valine codon (GTC) at position 191, which was replaced with an alanine codon (GCC); the second contains the target

valine codon (GTG) at position 485, which was replaced with an alanine codon (GCG). All mutations were confirmed by DNA sequencing

Cell transfection. Human embryonic kidney cells (HEK-293) were transiently transfected with pECFP-N1–CCR5wt alone or plus pEYFP-N1–CCR5wt, with pECFP-N1–CCR5mut alone or plus pEYFP-N1–CCR5mut, with PECFP-N1–CCR2wt alone or plus pEYFP-N1–CCR5wt, or with PECFP-N1–CCR2wt plus pEYFP-N1–CCR5mut constructs using Lipofectamine (Gibco-BRL) according to manufacturer's instructions. Mouse L1.2 cells were transfected by electroporation (1,170 μF, 310 V) with human CCR5wt, CCR5I52VV150A, CCR2wt or CCR2V64AV164A cDNA cloned in pcDNAIII. Stably transfected cells were selected in G-418 (Gibco-BRL) and screened by flow cytometric analysis for receptor expression with anti-CCR5 or anti-CCR2. All experiments were done with at least four cell lines for each plasmid.

Flow cytometric analysis and confocal microscopy. Cells were centrifuged (250g, 10 min, 24 °C), plated in V-bottom 96-well plates (2.5×10^5 cells/well) and incubated with biotin-labeled CCR5-03 mAb (1 μg/50 μl/well, 60 min, 4 °C) or biotin-labeled CCL5 (R&D Systems) according to manufacturer's protocols. Cells were washed twice in PBS with 2% bovine serum albumin (BSA) and 2% FCS and centrifuged (250 g, 5 min, 4 °C). Fluorescein isothiocyanate–labeled streptavidin (Southern Biotechnologies) was added and incubated (30 min, 4 °C), plates washed twice, and cell-bound fluorescence determined in a Profile XL flow cytometer (525 nm; Coulter). Peptide incorporation in the cell membrane was analyzed by treating cells with biotin-labeled synthetic peptides (R5wt1 + R5wt4, or R5mut1 + R5mut4; 50 μg/ml, 30 min, 37 °C). Secondary antibody and flow cytometry were as above. For confocal microscopy analysis, cells were treated with biotin-labeled synthetic peptides, stained as above and developed with Cy2-streptavidin (Amersham Biotech); staining also included Cy3-labeled CCR5-03 mAb. Images were captured with the Olympus 60X1-4 PlanApo objective of a Bio-Rad Radiance 2000 MP confocal microscope (Ar, 488 nm; He-Ne, 543 nm; red laser diode, 637 nm) mounted on an Olympus IX70. Cy2 fluorescence was captured with an HQ515/30 emission filter after sample excitation at 488 nm. Cy3 fluorescence was captured independently of Cy2 after excitation at 543 nm, with an HQ600/50 emission filter (DCLPXR 560 dichroic mirror); final images resulted from coupling of the individual images.

CTx and CCR5 costaining. HEK-293 cells, which constitutively express TfR, were transiently transfected with CCR5wt or CCR5mut and incubated (30 min, 12 °C) with anti-CCR5 or anti-TfR (Calbiochem), followed by Cy3–goat anti-mouse (Jackson Laboratories) and FITC-CTx (Sigma; 30 min, 12 °C). Cells were fixed (5 min, on ice) with 3.7% paraformaldehyde in PBS, followed by methanol (10 min, –20 °C), before mounting in Vectashield medium (Vector Labs), and visualized by confocal laser scanning microscopy (Leica). Signal intensity for each fluorophore was covered by a linear scale of pixel intensities. Digital images were processed with Photoshop software (Adobe Systems).

Binding analysis. Competition binding assays were carried out with CCR5wt– and CCR5mut–stably transfected L1.2 cells (0.5×10^6 cells/well) using 0.15 nM ^{125}I-labeled CCL5 (2,000 Ci/mmol; Amersham Pharmacia) as tracer and unlabeled CCL5 (0.19–250 nM)[49].

Calcium determination. Changes in intracellular Ca^{2+} concentration were monitored with the fluorescent probe Fluo-3AM (Calbiochem). Cells were treated as described[18] and Ca^{2+} mobilization in response to CCL5 (20 nM; PeproTech) determined at 37 °C in an EPICS XL flow cytometer at 525 nm (Coulter). Background stabilization and probe levels were determined for each sample. When necessary, we used hCCR4–, hCCR6–, hCCR8–, hCCR9– or hCCR10–stably transfected HEK-293 cells (a gift of J. Gutierrez, CNB, Madrid) and J-HM1-2.2 cells[30].

When the effect of synthetic peptides was analyzed, cells were pretreated with peptides (50 μg/ml, 30 min, 37 °C) before stimulation.

***In vitro* and *in vivo* cell migration assays.** For *in vitro* assays, cells (0.25×10^6 cells in 0.1 ml) were placed in the upper well of 24-well transmigration chambers (5-μm pore; Transwell; Costar) whose membrane was precoated with type VI collagen (Sigma; 20 μg/ml). CXCL12, CCL5 or CCL2 (PeproTech) were then added at different concentrations (in 0.6 ml RPMI with 0.25% BSA) to the lower well. Plates were incubated (120 min, 37 °C) and cells that migrated to the lower chamber were counted as described[18].

For *in vivo* assays, human PBLs were activated with PHA (50 μg/ml; Roche Diagnostics) and rIL-2 (20 ng/ml) for 4–6 d until they expressed a functional CCR5, as confirmed by anti-CCR5 staining and *in vitro* chemotaxis. Subsequently, 10^7 cells/ml were stained with Cell Tracker orange (Molecular Probes) (2.5 μM, 45 min, 37 °C) and 10^7 cells/ml with Cell Tracker green (Molecular Probes) (3 μM, 45 min, 37 °C), and washed. Green-stained cells (2×10^6 cells/ml) were treated with WT pep (50 μg/ml, 30 min, 37 °C) or with PBS (control); orange-stained cells (2×10^6 cells/ml) were treated with Mut pep (50 μg/ml, 30 min, 37 °C) or PBS. PBS + PBS– or WT pep + Mut pep–treated cell mixtures (1:1 orange/green; total 2×10^7 cells/200 μl in PBS) were injected intravenously into 5-month-old BALB/c mice; immediately thereafter, each mouse received an intrasplenic injection of CCL5 (1 μg/mouse in 75 μl) or PBS. After 4 h, mice were killed, spleens removed, erythrocytes lysed and fluorophore-labeled cells counted by flow cytometry. Migration index was calculated as the number of $CCR5^+$ cells that migrated in response to CCL5 compared with those that migrated to PBS, and expressed as mean ± s.d. The ratio of orange-stained to green-stained cells was calculated as the number of each population versus the total number of migrated cells.

Immunoprecipitation, immunoblotting and receptor cross-linking assays. Serum-starved cells were left unstimulated or stimulated (1 and 5 min, 37 °C) with CCL5 (20 nM). After washing twice with cold (4 °C) PBS, 10 μl of 100 mM DSS (Pierce) was added (10 min, 4 °C, with continuous rocking). Cell lysates were immunoprecipitated with anti-CCR5 and transferred to nitrocellulose membranes, as described[50]. The immunoblot was analyzed with CCR5 mAb. Each experiment was performed at least five times.

Peptide synthesis. The peptides WT pep and Mut pep were synthesized on an automated multiple synthesizer (AMS 422, Abimed) with the solid-phase procedure and standard Fmoc chemistry[51]. Peptide purity and composition were confirmed in reverse-phase high-performance liquid chromatography on a C-18 Nucleosil 120 analytical column with a 5%–70% acetonitrile gradient containing 1% trifluoracetic acid, as well as by amino acid analysis on a Beckman 6300 amino acid analyzer after acid hydrolysis, and by mass spectrometry with an ion-trap mass spectrometer, model LCQ, with an electrospray interface (ThermoQuest).

Fluorescence microscopy analysis. HEK-293 cells transiently transfected with CCR5-CFP–CCR5-YFP or CCR5mut-CFP–CCR5mut-YFP, either unstimulated or chemokine stimulated (5 min, 37 °C), were fixed with cold 4% formaldehyde in PBS (5 min). Fluorescence was visualized with a 100×, 1.3-NA oil objective on an inverted fluorescence microscope (Olympus IX70, 100-W Hg lamp). CFP was observed under a 435/10-nm excitation filter, 455-nm dichroic beam splitter and a 480/20-nm emission filter. YFP was viewed under a filter set with a 500/20-nm excitation filter, a 515-nm dichroic beam splitter and a 535/30-nm emission filter.

FRET was detected with 435/10-nm excitation, a 455-nm dichroic beam splitter and 535/30-nm emission filters. Images were captured with a cooled CoolView CCD camera (Photonic Science).

FRET measurement. FRET between CFP and YFP was determined from the whole image on a pixel-by-pixel basis by a three-filter method[27,52,53]. Briefly, we calculated autofluorescence as well as CFP and YFP bleed-through on the FRET channel, which showed 54.30 ± 0.22% CFP and 1.1 ± 0.05% YFP fluorescence bleed-through to the FRET channel. To calculate cross-talk in these experiments, values for CFP and YFP images were multiplied by 0.545 and 0.012, respectively. The corrected FRET image (FRETC) was obtained by subtracting autofluorescence and bleed-through from original FRET images. The final FRETC image is presented as a quantitative pseudocolor image. Background was subtracted before other image treatments were done. For quantification, normalized FRET was calculated on the colocalization areas of CFP-CCR5 and YFP-CCR5 on a pixel-by-pixel basis[54]. Images were processed and FRET calculated with a program based on Visual Basic 6.0 (Microsoft). FRET was calculated for at least 30 cells each in seven independent experiments.

When the effect of synthetic peptides was analyzed by FRET, transfected HEK-293 cells were pretreated with peptides (50 μg/ml, 30 min, 37 °C) before stimulation.

Fluorescence lifetime imaging (FLIM) measurement. FLIM was determined in live, transiently-transfected cells cultured in coverslip chambers (Nunc). FLIM measurements were done with a Nikon confocal C1 microscope with a High Speed Lifetime Module and 60° PlanApo 1.4 objective. Fluorescence lifetime was determined after excitation with a 440-nm pulsed laser (picosecond pulses) and a 470/20-nm band-pass emission filter and quantified with LIMO software (Nikon). Lifetime values were obtained for 5 independent experiments of at least 15 cells each.

Note: Supplementary information is available on the Nature Immunology website.

ACKNOWLEDGMENTS

We thank J.P. Albar for peptide synthesis, J. Gutiérrez for chemokine receptor transfectants, M.C. Moreno-Ortíz for help with FACS analysis, and C. Bastos and C. Mark for secretarial and editorial assistance, respectively. Partially supported by grants from the Spanish Comisión Interministerial de Ciencia y Technologia and from the Ministry of Health. The Department of Immunology and Oncology was founded and is supported by the Spanish Council for Scientific Research (CSIC) and by Pfizer.

COMPETING INTERESTS STATEMENT

The authors declare that they have no competing financial interests.

Received 10 October; accepted 20 November 2003
Published online at http://www.nature.com/natureimmunology/

1. Mackay, C.R. Chemokines: immunology's high impact factors. *Nat. Immunol.* **2**, 95–101 (2001).
2. Rossi, D. & Zlotnik, A. The biology of chemokines and their receptors. *Annu. Rev. Immunol.* **18**, 217–242 (2000).
3. Mellado, M., Rodríguez-Frade, J.M., Mañes, S. & Martinez-A., C. Chemokine signaling and functional responses: the role of receptor dimerization and TK pathway activation. *Ann. Rev. Immunol.* **19**, 397–421 (2001).
4. Angers, S., Salahpour, A. & Bouvier, M. Dimerization: an emerging concept for G protein-coupled receptor ontogeny and function. *Annu. Rev. Pharmacol. Toxicol.* **42**, 409–435 (2002).
5. Hebert, T.E. *et al.* A peptide derived from a β2-adrenergic receptor transmembrane inhibits both receptor dimerization and activation. *J. Biol. Chem.* **271**, 16384–16392 (1996).
6. Zeng, F.Y. & Wess, J. Identification and molecular characterization of m3 muscarinic receptor dimers. *J. Biol. Chem.* **274**, 19487–19497 (1999).
7. Kaupmann, K *et al.* $GABA_B$-receptor subtypes assemble into functional heteromeric complexes. *Nature* **396**, 683–687 (1998).
8. Galvez, T. *et al.* Allosteric interactions between GB1 and GB2 subunits are required for optimal GABA(B) receptor function. *EMBO J.* **20**, 2152–2159 (2001).
9. Milligan, G. Oligomerization of G-protein-coupled receptors. *J. Cell Sci.* **114**, 1265–1271 (2002).
10. Tsuji Y. *et al.* Cryptic dimer interface and domain organization of the extracellular region of metabotropic glutamate receptor subtype 1. *J. Biol. Chem.* **275**, 28144–28151 (2000).
11. White J. H. *et al.* Heterodimerization is required for the formation of a functional $GABA_B$ receptor. *Nature* **396**, 679–682 (1998).
12. Filizola, M. & Weinstein, H. Structural models for dimerization of G-protein coupled receptors: the opioid receptor homodimers. *Biopolymers* **66**, 317–325 (2002).
13. Benkirane, M., Jin, D.Y., Chun, R.F., Koup, R.A. & Jeang, K.T. Mechanism of transdominant inhibition of CCR5-mediated HIV-1 infection by ccr5Δ32. *J. Biol. Chem.* **272**, 30603–30606 (1997).
14. Issafras, H. *et al.* Constitutive agonist-independent CCR5 oligomerization and antibody-mediated clustering occurring at physiological levels of receptors. *J. Biol. Chem.* **277**, 34666–34673 (2002).
15. Babcock, G.J., Farzan, M. & Sodroski, J. Ligand-independent dimerization of CXCR4, a principal HIV-1 coreceptor. *J. Biol. Chem.* **278**, 3378–3385 (2003).
16. Blanpain, C. *et al.* Multiple active states and oligomerization of CCR5 revealed by functional properties of monoclonal antibodies. *Mol. Biol. Cell* **13**, 723–737 (2002).
17. Rodríguez-Frade, J.M., Mellado, M. & Martínez-A., C. Chemokine receptor dimerization: two are better than one. *Trends Immunol.* **22**, 612–617 (2001).
18. Mellado, M. *et al.* Chemokine receptor homo- or hetero-dimerization activates distinct signaling pathways. *EMBO J.* **20**, 2497–2507 (2001).
19. Vila-Coro, A.J. *et al.* HIV-1 infection through the CCR5 receptor is blocked by receptor dimerization. *Proc. Natl. Acad. Sci. USA* **97**, 3388–3393 (2000).
20. Gobel, U., Sander, C., Schneider, R. & Valencia, A. Correlated mutations and residue contacts in proteins. *Proteins* **18**, 309–317 (1994).
21. Pazos, F. & Valencia, A. *In silico* two-hybrid system for the selection of physically interacting protein pairs. *Proteins* **47**, 219–227 (2002).
22. Casari, G., Sander, C. & Valencia, A. A method to predict functional residues in proteins. *Nat. Struct. Biol.* **2**, 171–178 (1995).
23. del Sol Mesa, A., Pazos, F. & Valencia, A. Automatic methods for predicting functionally important residues. *J. Mol. Biol.* **326**,1289–1302 (2003).
24. Manes, S. *et al.* Membrane raft microdomains mediate front-rear polarity in migrating cells. *EMBO J.* **18**, 6211–6220 (1999).
25. Harder, T., Scheiffele, P., Verkade, P. & Simons, K. Lipid domain structure of the plasma membrane revealed by patching of membrane components. *J. Cell Biol.* **141**:929–942 (1998).
26. Kenworthy, A.K. Imaging protein-protein interactions using fluorescence resonance energy transfer microscopy. *Methods* **24**, 289–296 (2001).
27. Gordon, G.W., Berry, G., Liang, X.H., Levine, B. & Herman, B. Quantitative fluorescence resonance energy transfer measurements using fluorescence microscopy. *Biophys. J.* **74**, 2702–2713 (1998).
28. Bastiaens, P.I. & Squire, A. Fluorescence lifetime imaging microscopy: spatial resolution of biochemical processes in the cell. *Trends Cell Biol.* **9**, 48–52 (1999).
29. Angers, S. *et al.* Detection of β2-adrenergic receptor dimerization in living cells using bioluminescence resonance energy transfer (BRET) *Proc. Natl. Acad. Sci. USA* **97**, 3684–3689 (2000).
30. Desai, D.M., Newton, M.E., Kadlecek, T. & Weiss A. Stimulation of the phosphatidylinositol pathway can induce T-cell activation. *Nature* **348**,66-69 (1990).
31. Klemm, J.D., Schreiber, S.L. & Crabtree, G.R. Dimerization as a regulatory mechanism in signal transduction. *Annu. Rev. Immunol.* **16**, 569-592 (1998).
32. Devi, L. Heterodimerization of G-protein-coupled receptors: pharmacology, signaling and trafficking. *Trends Pharm. Sci.* **22**, 532–537 (2001).
33. Gether, U. Uncovering molecular mechanisms involved in activation of G protein-coupled receptors. *Endocrinol. Rev.* **21**, 90–113 (2000).
34. Ghanouni, P., Steenhuis, J.J., Farrens, D.L. & Kobilka, B.K. Agonist-induced conformational changes in the G protein-coupling domain of the β2 adrenergic receptor. *Proc. Natl. Acad. Sci. USA* **98**, 5997–6002 (2001).
35. Ri, Y. *et al.* The role of a conserved proline residue in mediating conformational changes associated with voltage gating of Cx32 gap junctions. *Biophys J.* **76**, 2887–2889 (1999).
36. Govaerts, C. *et al.* The TXP motif in the second transmembrane helix of CCR5. *J. Biol. Chem.* **276**, 13217–13225 (2001).
37. Soriano, S.F. *et al*, Chemokines integrate JAK/STAT and G protein pathways during chemotaxis and calcium flux responses. *Eur. J. Immunol.* **33**, 1328–1333 (2003).
38. Onuffer, J.J. & Horuk R. Chemokines, chemokine receptors and small-molecule antagonists: recent developments. *Trends Pharm. Sci.* **23**, 459–467 (2002).
39. Tarasova, N. I., Rice, W. G. & Michejda, C.J. Inhibition of G-protein-coupled receptor function by disruption transmembrane domain interactions. *J. Biol. Chem.* **274**, 34911–34915 (1999).
40. Dragic, T. *et al.* A binding pocket for small molecule inhibitor of HIV-1 entry within the transmembrane helices of CCR5. *Proc. Natl. Acad. Sci. USA* **97**, 5639–5644 (2000).
41. Mirzadegan, T *et al.* Identification of the binding site for a novel class of CCR2b chemokine receptor antagonists. *J. Biol. Chem.* **275**, 25562–25571 (2000).
42. Horn, F. *et al.* GPCRDB information system for G protein-coupled receptors. *Nucleic Acids Res.* **31**, 294–297 (2003).
43. Notredame, C., Higgins, D.G. & Heringa, J. T-Coffee: a novel method for fast and accurate multiple sequence alignment. *J. Mol. Biol.* **302**, 205–217 (2000).
44. Filizola, M., Olmea, O. & Weinstein, H. Prediction of heterodimerization interfaces of G-protein coupled receptors with a new subtractive correlated mutation method. *Protein Eng.* **15**, 881–885 (2002).
45. Palczewski, K. *et al.* Crystal structure of rhodopsin: a G protein–coupled receptor. *Science* **289**, 739–745 (2000).
46. Katchalski-Katzir, E. *et al.* Molecular surface recognition: determination of geometric fit between proteins and their ligands by correlation techniques. *Proc. Natl. Acad. Sci. USA* **89**, 2195–2199 (1992).
47. Vakser, I.A. & Jiang, S. Strategies for modeling the interactions of transmembrane helices of G protein-coupled receptors by geometric complementarity using the GRAMM computer algorithm. *Methods Enzymol.* **343**, 313–328 (2002).
48. Pazos, F., Helmer-Citterich, M., Ausiello, G. & Valencia, A. Correlated mutations contain information about protein-protein interaction. *J. Mol. Biol.* **271**, 511–523 (1997).
49. Gong, X. *et al.* Monocyte chemotactic protein-2 (MCP-2) uses CCR1 and CCR2B as its functional receptors. *J. Biol. Chem.* **272**,11682–11685 (1997).
50. Mellado, M. *et al.* The chemokine MCP-1 triggers tyrosine phosphorylation of the CCR2B receptor and the JAK2/STAT3 pathway. *J. Immunol.* **161**, 805–813 (1998).
51. Gausepohl, H. *et al.* Automated multiple peptide synthesis. *Peptide Res.* **5**, 315–320 (1992).
52. Sorkin, A., McClure, M., Huang, F. & Carter, R. Interaction of EGF receptor and grb2 in living cells visualized by fluorescence visualized by fluorescence resonance energy transfer (FRET) microscopy. *Curr. Biol.* **10**, 1395–1398 (2000).
53. Gu, C., Cali, J.J. & Cooper, D.M. Dimerization of mammalian adenylate cyclases. *Eur. J. Biochem.* **269**, 413–421 (2002).
54. Xia, Z. & Liu, Y. Reliable and global measurement of fluorescence resonance energy transfer using fluorescence resonance energy transfer (FRET) microscopy. *Biophys. J.* **81**, 2395–4028 (2001).